

Supporting Information

Morphology Controlled Cu_3BiS_3 Nanostructures: Superior Electrocatalytic Sensing of organic nitro compounds

Manzoor Ahmad Pandit^{a,b,§}, Dasari Sai Hemanth Kumar^{b,§}, Mohan Varkolu^{b,c}, and Krishnamurthi Muralidharan^{b,*}

^aMaterials Genome Institute, Shanghai University, Shanghai 200444, China.

^bSchool of Chemistry, University of Hyderabad, Hyderabad 500046, India.

^cDepartment of Chemistry, College of Engineering, Koneru Lakshmaiah Education Foundation, RVS Nagar, Azziz Nagar (PO), Moinabad Road, Hyderabad-500075, Telanagana, India.

*Email: murali@uohyd.ac.in

§Both the authors contributed equally.

S. No.	Title	Page no.
S1	High magnification FESEM and SAED patterns of Cu_3BiS_3 with DBU, DABCO and DBN as bases.	2
S2	Average particle size distribution plots	2
S3	EDAS of Cu_3BiS_3 .	3
S4	BJH plots of Cu_3BiS_3 nanomaterials.	3
S5	UV-visible DRS of Cu_3BiS_3 .	4
S6	CV in the absence and presence of 4-NP, and linear plots of scan rate vs. current for the three morphologies-spheres, rods, and worms.	4
S7	CV at different pH with 2,4-DNP for the three different morphologies. The linear fit responses of different pH (5 - 9).	5
S8	CV at different scan rates with 2,4-DNP. The corresponding linear plots of scan rates vs. current of 2,4-DNP.	5
S9	The corresponding current vs. concentration linear plots of 4-NP and 2,4-DNP for three catalysts.	6
S10	Interference studies for three catalysts catalysts spheres, rods, and worms respectively.	6

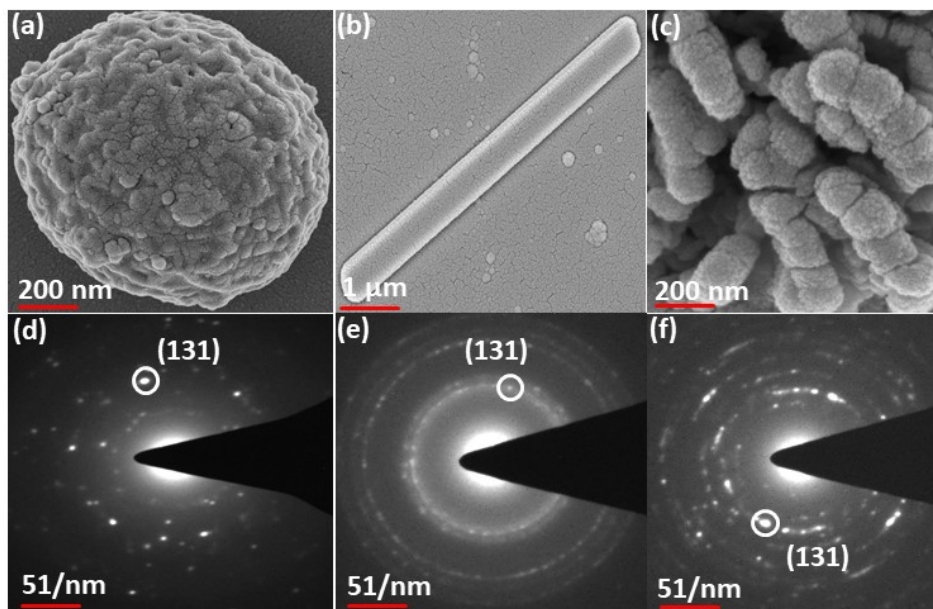


Figure S1. Showing high magnified FESEM and SAED patterns of Cu_3BiS_3

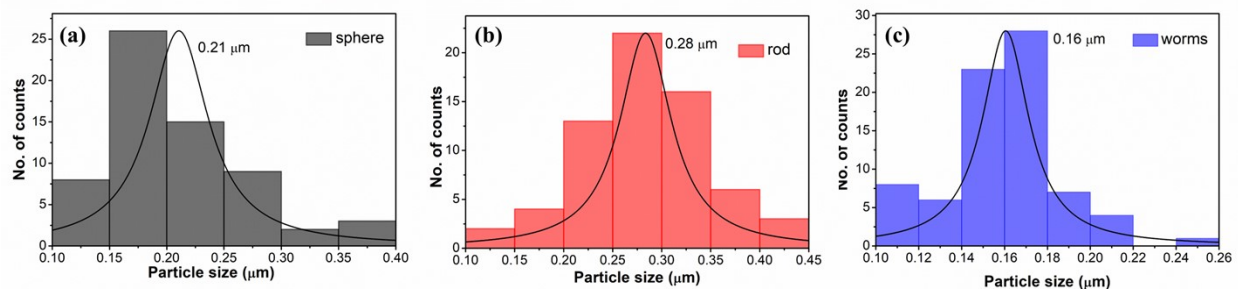


Figure S2. Average particle size distribution plots of (a) Spheres of Cu_3BiS_3 -DBU, (b) rods of Cu_3BiS_3 -DABCO, (c) worm-like morphology of Cu_3BiS_3 -DBN.

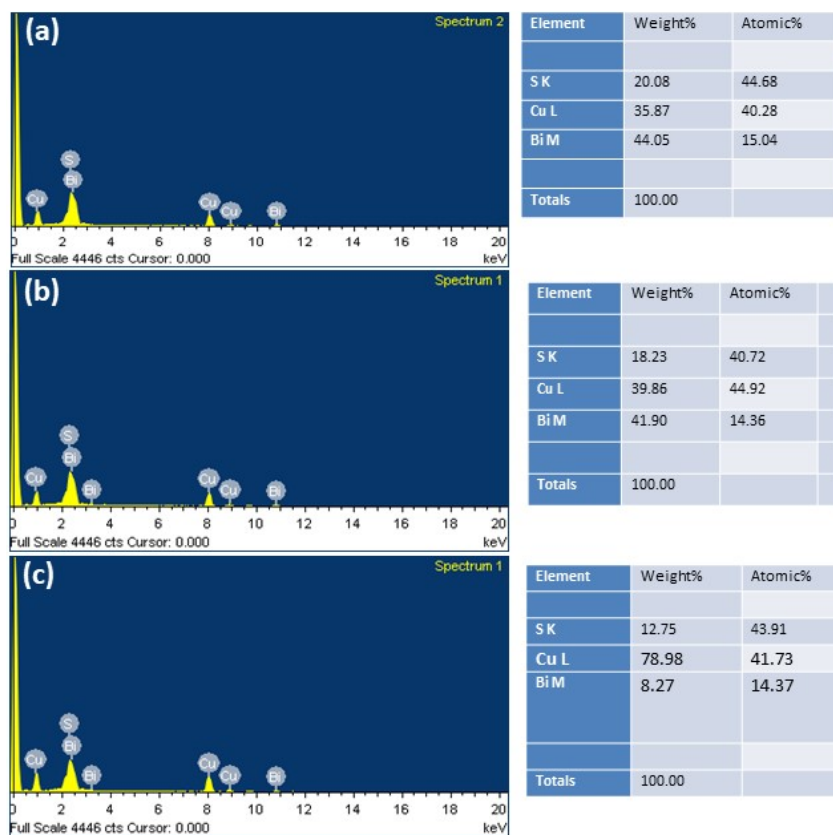


Figure S3. Showing EDAS of (a) spheres, (b) rods, and (c) worms of Cu_3BiS_3 catalysts

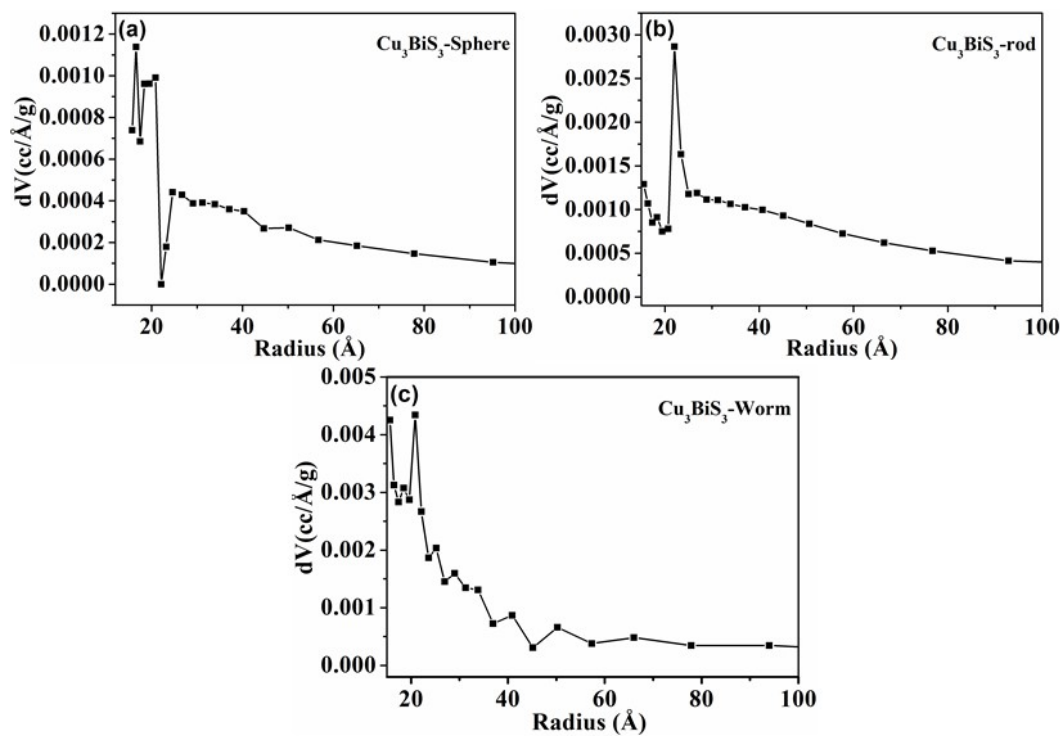


Figure S4. BJH plots representing pore size distribution of Cu_3BiS_3 nanomaterials.

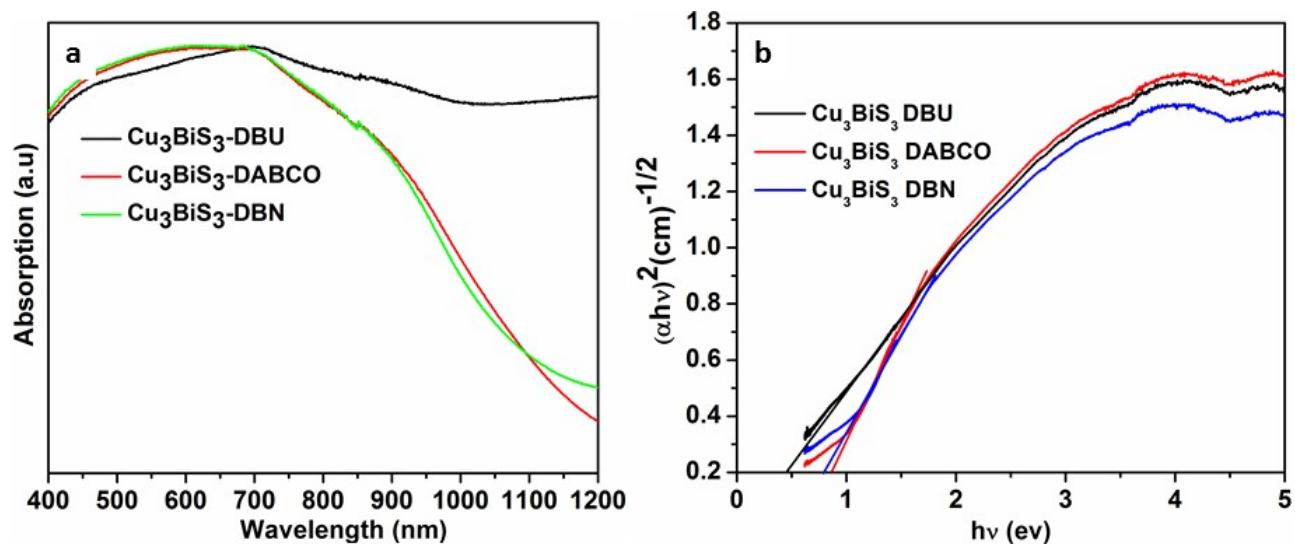


Figure S5. Showing UV-visible DRS system of Cu_3BiS_3 (a) Absorption spectrum (b) band gap.

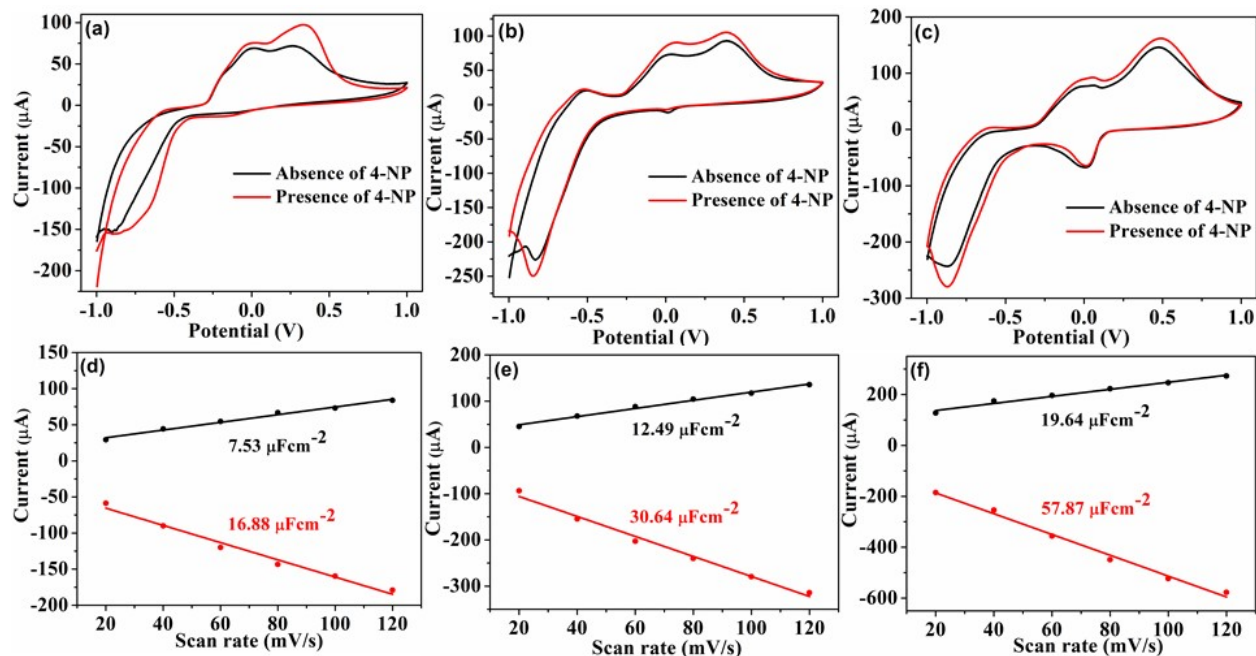


Figure S6. (a-c) CV in the absence and presence of 4-NP for the three different morphologies-spheres, rods, and worms. (d-f) Linear plots of scan rate vs. current.

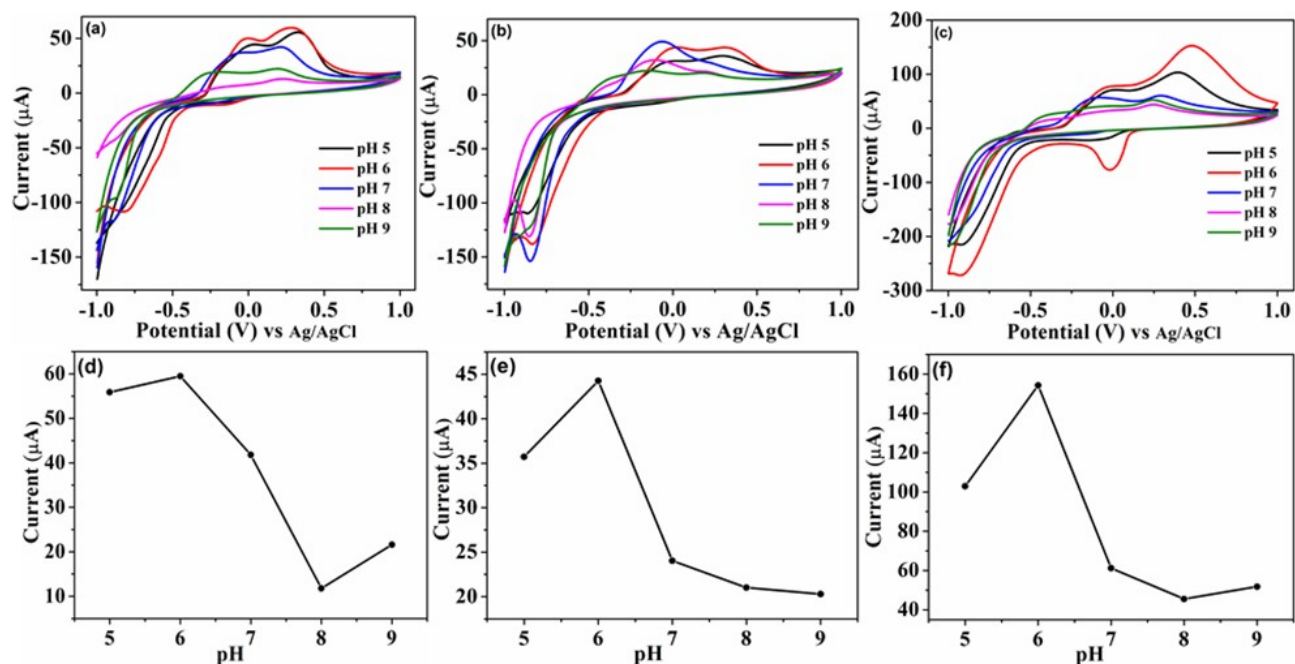


Figure S7. (a-c) CV at different pH with 2,4-DNP for the three different morphologies-spheres, rods, and worms. (d-f) The linear fit responses of different pH (5 - 9) for the three morphologies.

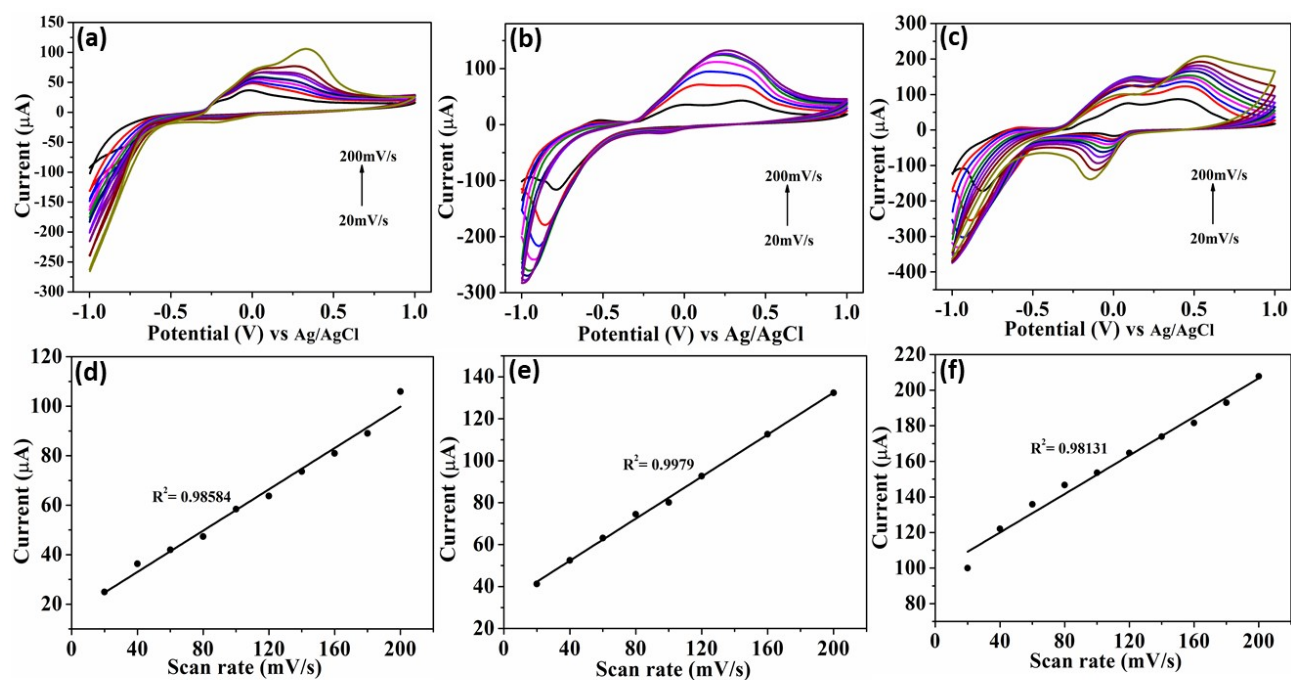


Figure S8. (a-c) CV of Cu_3BiS_3 with 2,4-DNP at different scan rates. (d-f) The corresponding linear plots of scan rates vs current of 2,4-DNP.

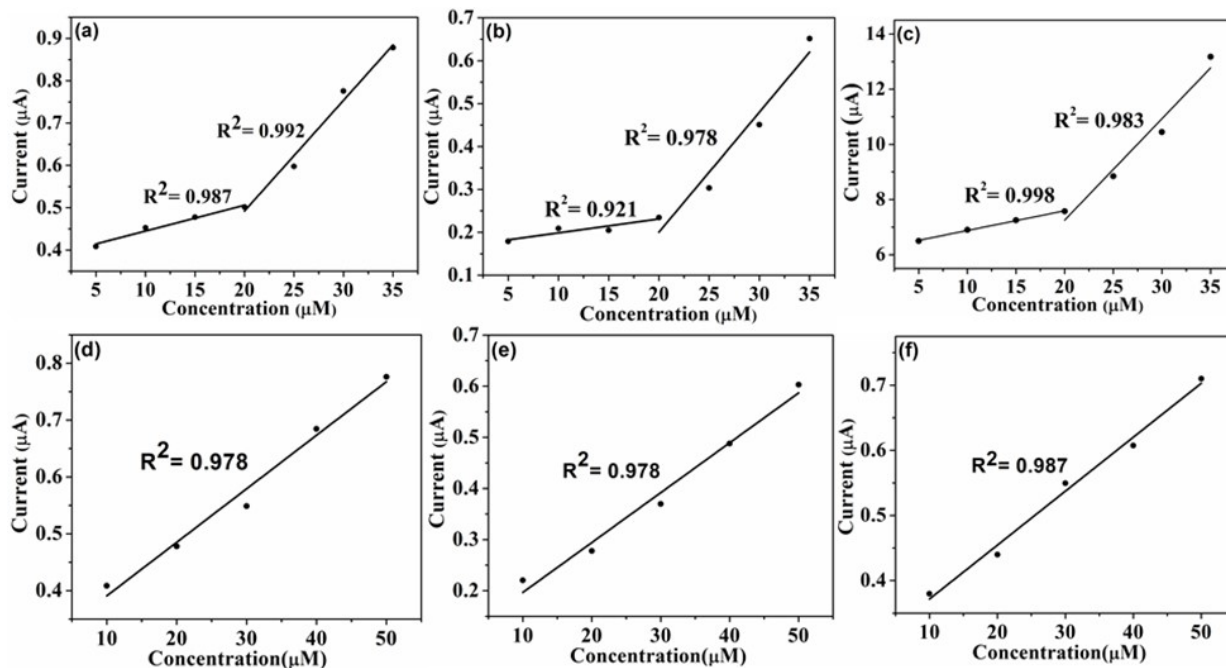


Figure S9. The corresponding current vs. concentration linear plots of (a-c) 4-NP, and (d-f) 2,4-DNP for three catalysts spheres, rods, and worms respectively.

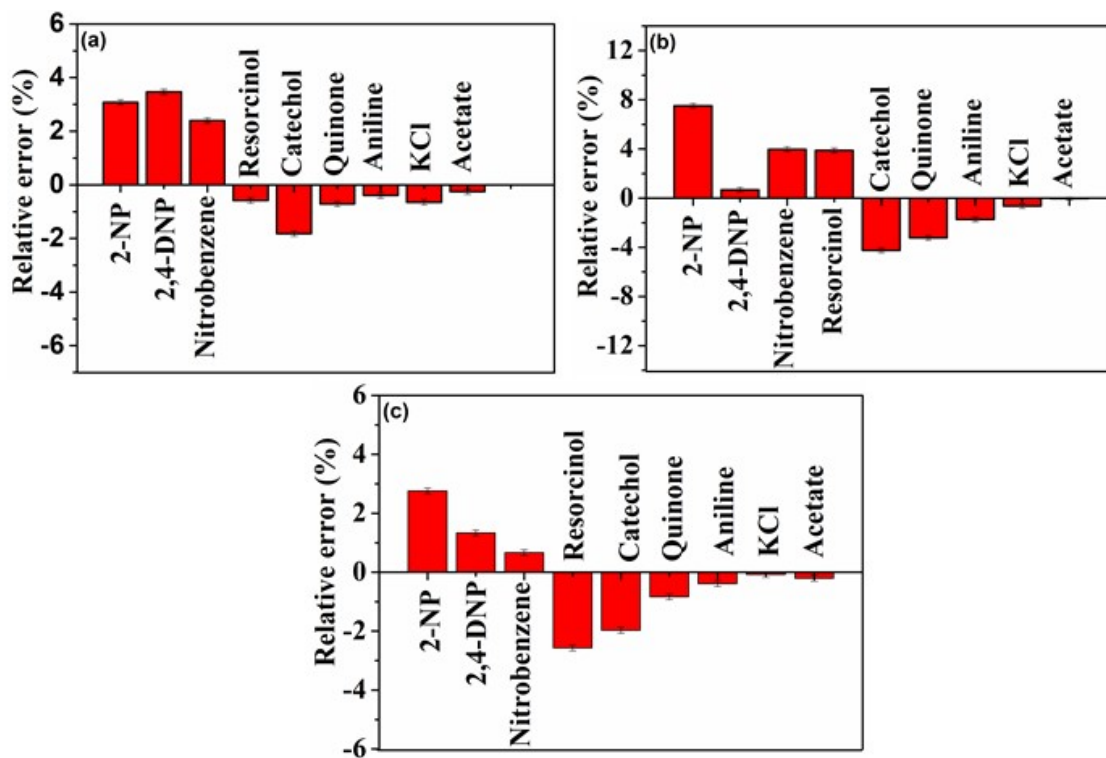


Figure S10. Interference studies for three Cu_3BiS_3 catalysts: spheres, rods, and worms respectively.